

Supporting Information

A Versatile and Low-Toxic Material for Photothermal Therapy in Deeper Tissues

Liguo Jin,^{†, ‡} Yinyin Wang,[‡] Huan Ouyang,[‡] Yu Liu,[‡] Zhenling Zhu,^{†, ‡} Shuhua Wang,[†]

Hongbo Xin,[‡] Xiaolei Wang*,^{†, ‡}

[†]College of Chemistry, Nanchang University, Nanchang, Jiangxi 330088, P.R. China.

[‡]The National Engineering Research Center for Bioengineering Drugs and the Technologies:

Institute of Translational Medicine, Nanchang University, Nanchang, Jiangxi 330088, P.R. China.

Corresponding Author

* E-mail: wangxiaolei@ncu.edu.cn Tel: 0791-83827416.

Table of contents

1. Experimental procedures

1.1 Materials

1.2 Synthesis of TPUU

1.3 Characterizations of TPUU

1.4 Synthesis of Au-Ns

1.5 Characterizations of Au-Ns

1.6 Agar-simulated experiments

1.7 The ability to release drugs

1.8 Photothermal effect of Au-Ns

1.9 Hemolysis assay

1.10 Cells culture

1.11 Cytotoxicity assay

1.12 Animal experiments

1.13 Quantitative real-time polymerase chain reaction (RT-qPCR)

1.14 Quantitative 16S ribosomal DNA (16S rDNA)

1.15 Statistical analysis

2. Supplementary Figures

2. Supplementary Figures

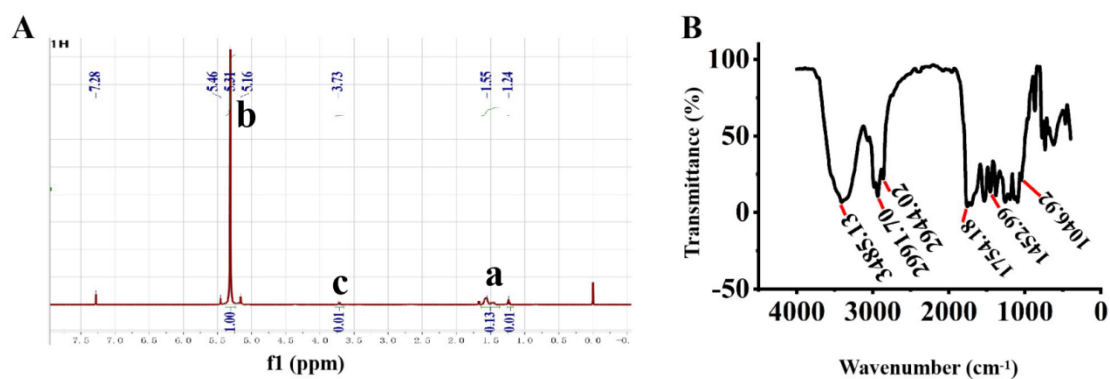


Fig. S1. A. ^1H NMR spectrum of PDLLA; **B.** FTIR spectrum of PDLLA.

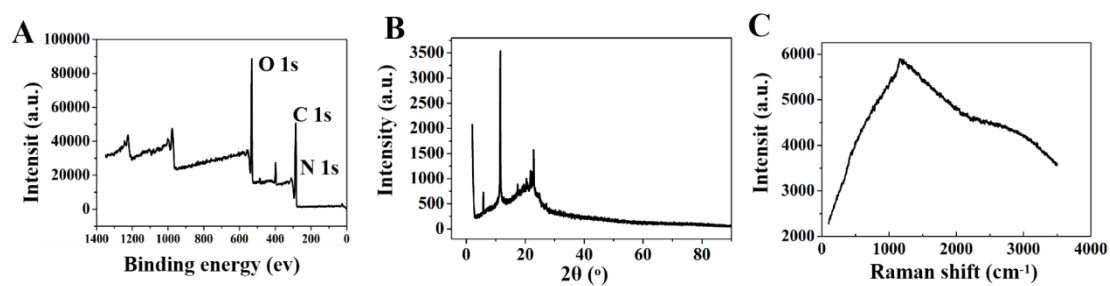


Fig. S2. A. XPS spectrum of TPUU; **B.** XRD analysis of TPUU; **C.** Raman spectrum of TPUU.

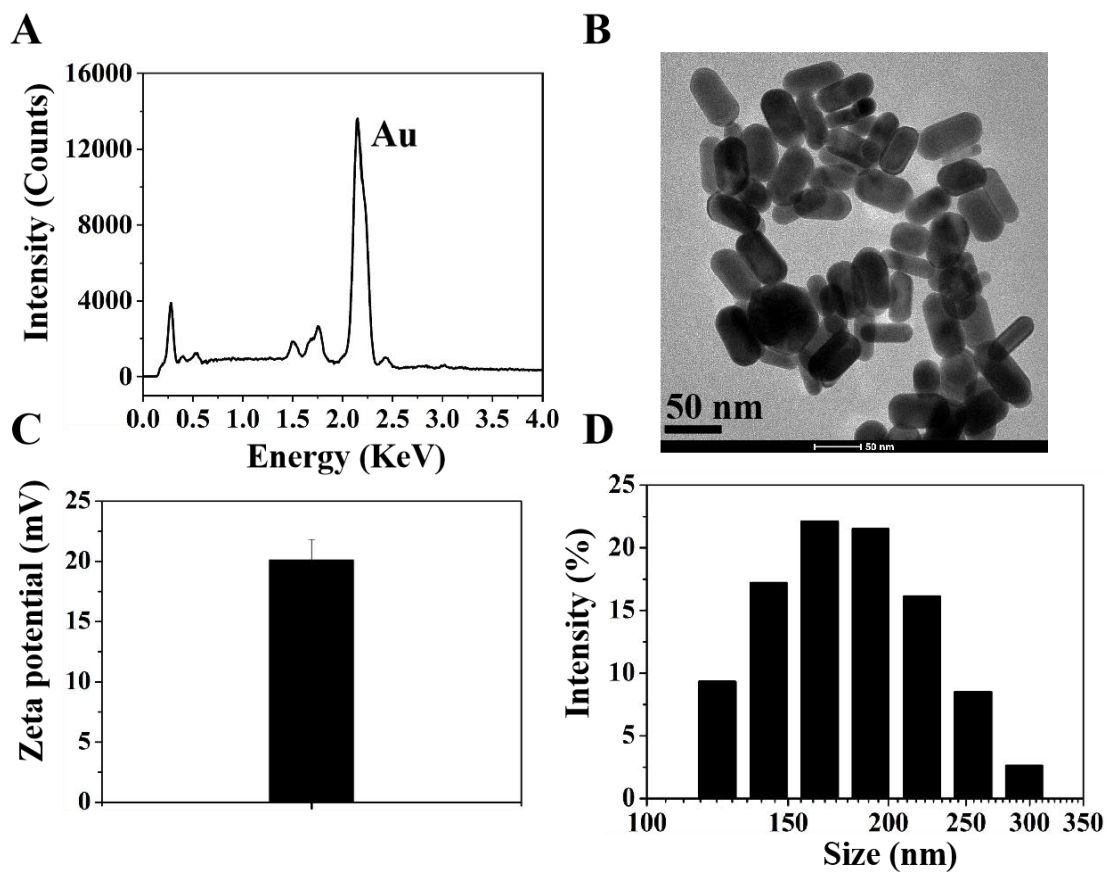


Fig. S3. **A.** EDS spectrum analysis of Au-Ns; **B.** TEM images of Au-Ns (Scale bar = 50 nm); **C.** Zeta potential of Au-Ns. **D.** Particle size of Au-Ns.

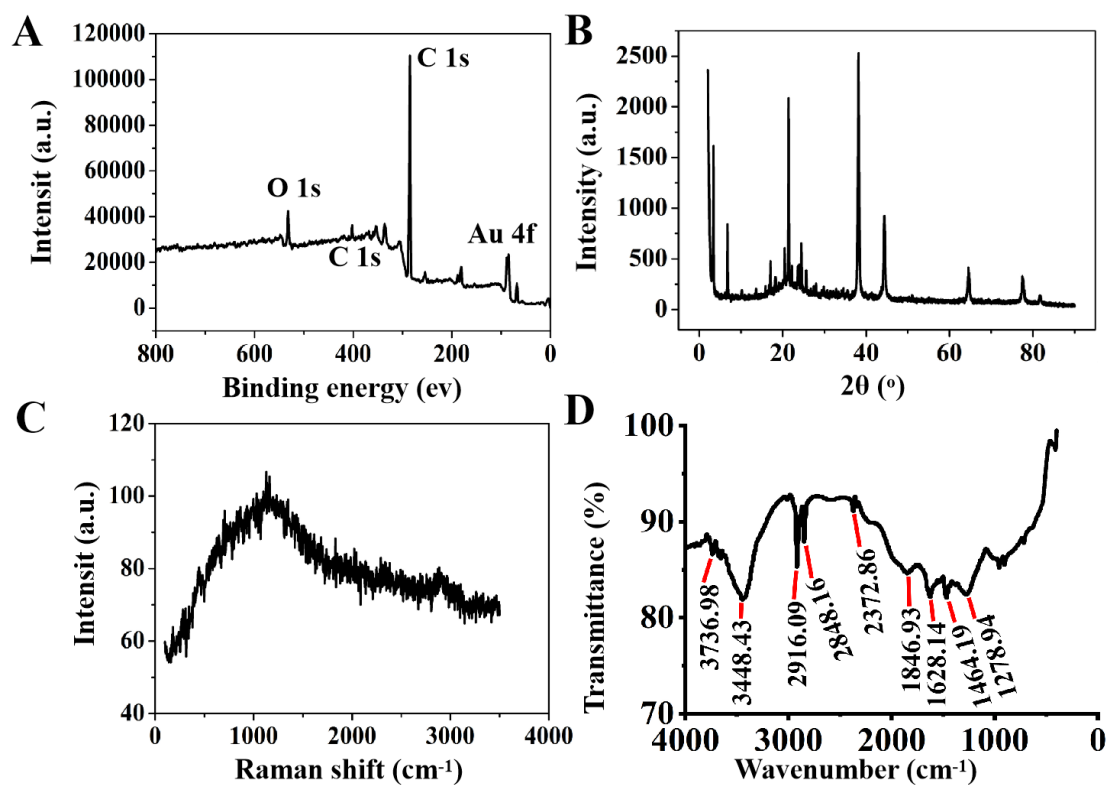


Fig. S4. **A.** XPS spectrum of Au-Ns; **B.** XRD analysis of Au-Ns; **C.** Raman spectrum of Au-Ns; **D.** FTIR spectrum of Au-Ns.

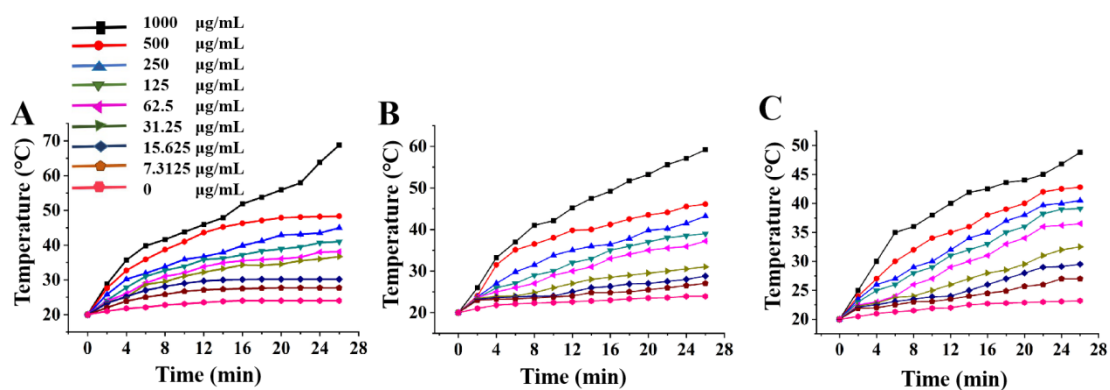


Fig. S5. The photothermal effect of Au-Ns on water as a control. **(A)** 2 W/cm²; **(B)** 1.5 W/cm²; **(C)** 0.6 W/cm²

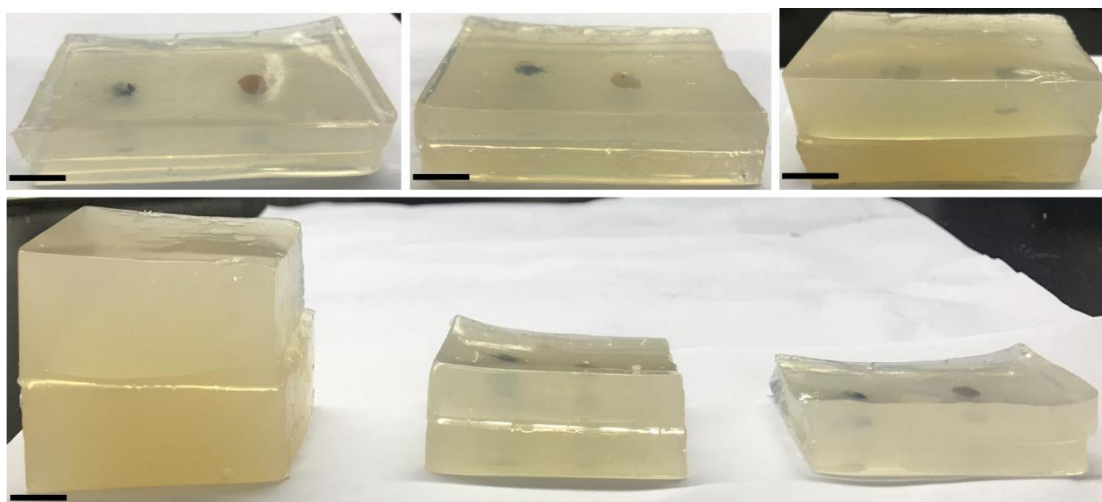


Fig. S6. Schematic representation of agar sandwiches. (Scale bar = 1 cm)

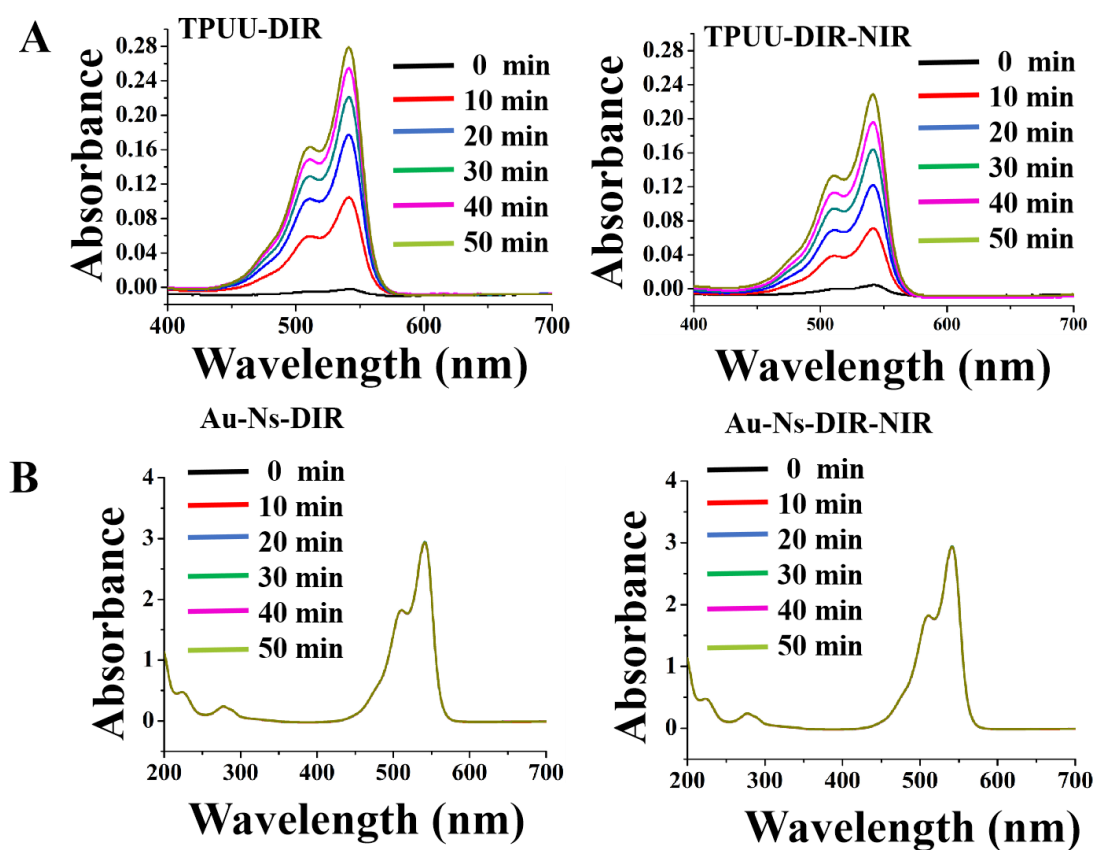


Fig. S7. Drugs release of DIR on TPUU and Au-Ns (DIR: 541 nm).

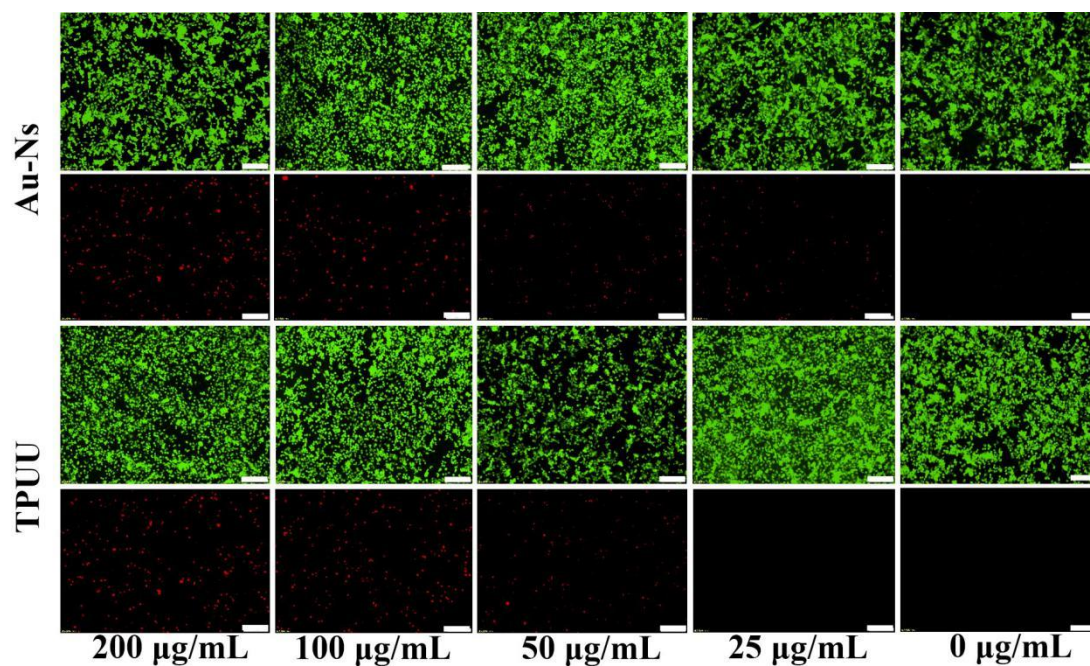


Fig. S8. Live/dead staining assay of 4T1 cells that were cultured in different concentrations for 24 h. Living cells and dead cells were stained with green and red fluorescence. (Scale bar = 100 μm).

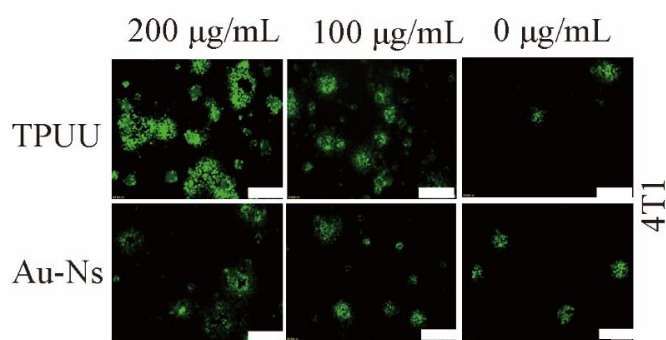


Fig. S9. The intracellular ROS content of 4T1 cells (Scale bar = 100 μm).

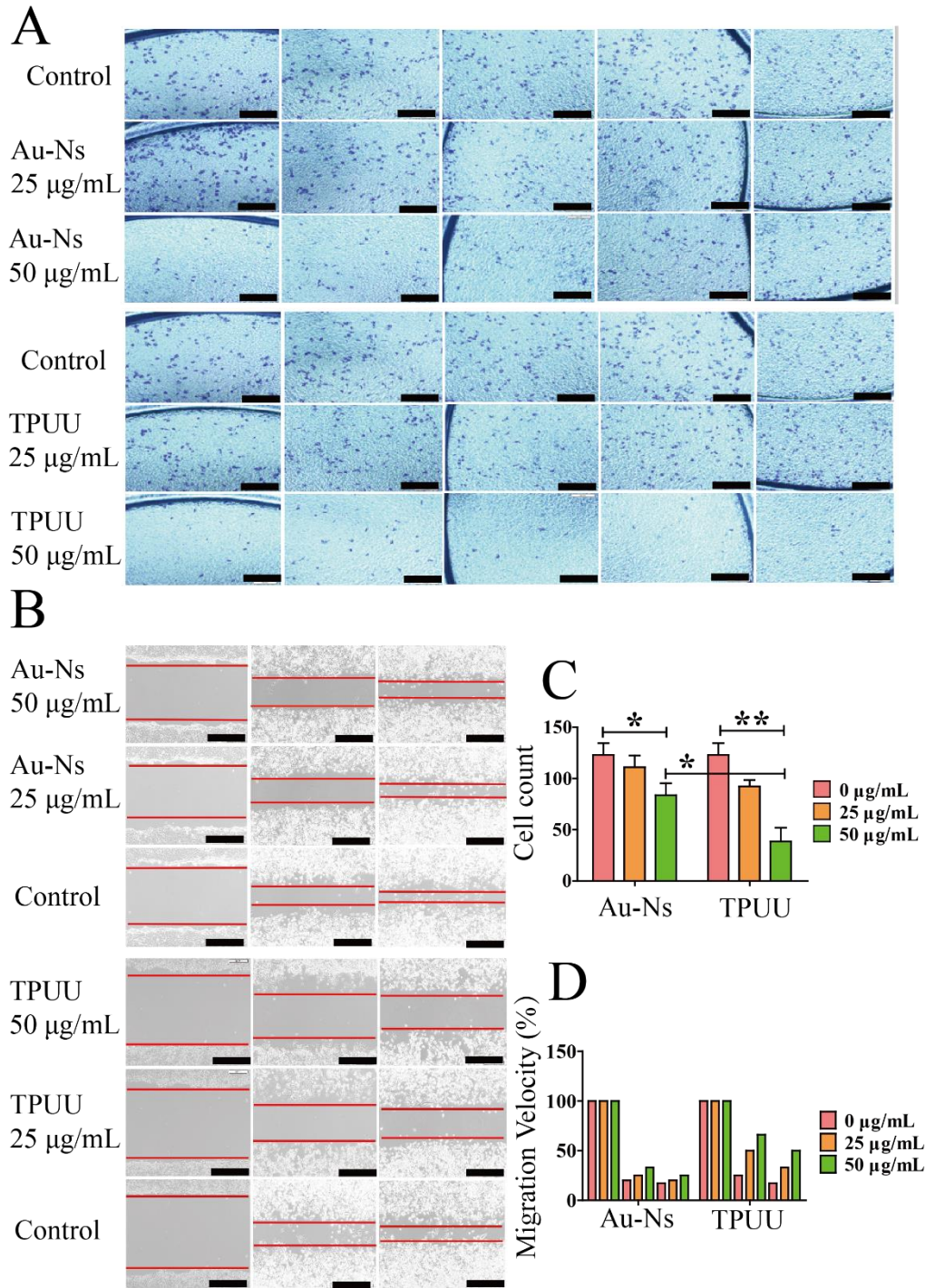


Fig. S10. Transwell assay of 4T1 cells that were cultured at different concentrations for 20 h (Scale bar = 100 µm). B. Scratch assay of 4T1 cells that were cultured with different concentrations for different time (Scale bar = 100 µm); C. Quantitative analysis of Transwell assay; D. Quantitative analysis of Scratch assay. (* $P < 0.05$, ** $P < 0.01$, *** $P < 0.001$. Error bars, SEM.)

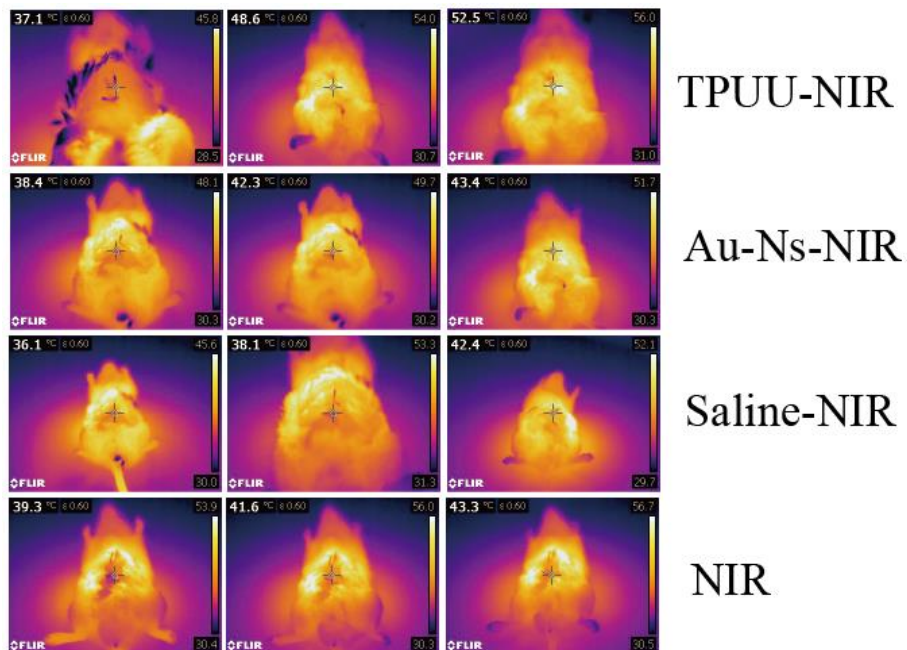


Fig. 11. The mouse intestine model was used to simulate the deep warming of TPUU *in vivo*, and photographed with an infrared camera under NIR irradiation.

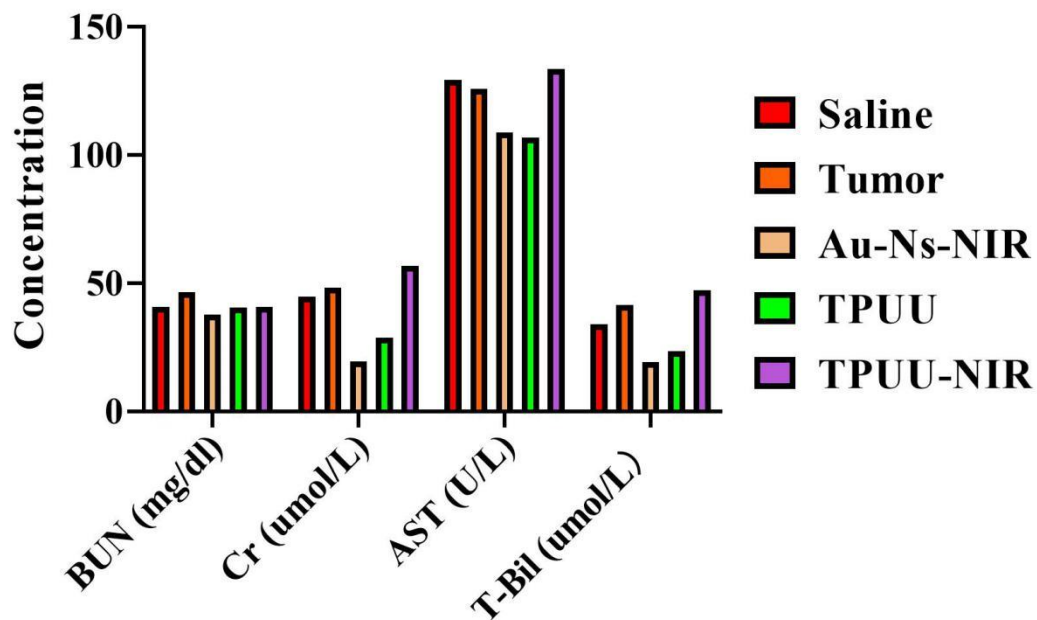


Fig. 12. Blood biochemical analysis of mice injected with the following groups: Saline, Tumor, Au-Ns-NIR, TPUU and TPUU-NIR.

	Normal Range	Saline	Tumor	TPUU	TPUU-NIR	Au-Ns-NIR
WBC	0.8-6.8 ($10^9/L$)	8.0	8.1	6.2	6.9	6.3
Lymph	0.7-5.7 ($10^9/L$)	6.3	6.7	5.0	4.8	4.3
Mon	0.0-0.3 ($10^9/L$)	0.2	0.2	0.2	0.3	0.4
Gran	0.1-1.8 ($10^9/L$)	1.5	1.2	1.0	1.8	1.6
Lymp %	55.8-90.6 (%)	78.7	82.2	80.7	69.1	69.0
Mon %	1.8-6.0 (%)	2.7	2.8	3.0	4.4	5.8
Gran %	8.6-38.9 (%)	18.6	15.0	16.3	26.5	25.2
RBC	6.36-9.42 ($10^{12}/L$)	5.08	5.92	9.60	5.78	9.33
HGB	110-143 (g/l)	162	154	149	149	152
HCT	34.6-44.6 (%)	26.4	33.3	47.6	29.8	47.3
MCV	48.2-58.3 (fl)	52.1	56.3	49.6	51.6	50.7
MCH	15.8-19 (pg)	31.8	26.0	15.5	25.7	16.2
MCHC	302-353 (g/l)	613	462	313	500	321
RDW	13-17 (%)	19.4	16.9	15.1	19.2	13.6
PLT	450-1590 ($10^9/L$)	1372	1003	877	1150	1040
MPV	3.8-6.0 (fl)	5.1	4.5	6.1	4.7	6.2
PDW		17.4	16.8	16.7	17.1	16.4
PCT	(%)	0.699	0.451	0.534	0.540	0.644

Table 1. Blood biochemistry analysis of mice injected with the following groups: Saline,

Tumor, Au-Ns-NIR, TPUU and TPUU-NIR.